AIChE

A Compact and High Throughput Reactor of Monolithic-Structured Catalyst Bed for Conversion of Syngas to Liquid Fuels

Wei Liu, Yong Wang, Wayne Wilcox, and Shari Li
Energy and Environmental Directorate, Pacific Northwest National Lab (PNNL), Richland, WA 99352

DOI 10.1002/aic.12797
Published online November 7, 2011 in Wiley Online Library (wileyonlinelibrary.com).

Syngas conversion is needed for the production of liquid fuels and/or chemicals from renewable or remote feedstock at capacities much smaller than the conventional Fischer–Tropsch (F–T) plant. Here, we present a multiscale-engineered, modular-type design approach toward the development of a compact reactor unit to make syngas-to-liquids economically feasible at small scales. The fundamental design idea is tested by using a Re-Co/alumina catalyst coated on a monolith support of channel size about 0.9 mm. One-pass CO conversion (92–98%) with 10% of CH_4 selectivity is obtained with the structured bed under typical F–T reaction conditions. The gas superficial linear velocity was found as one critical parameter that may allow scale-up of the hydrodynamics from the small-scale laboratory tests directly to practical sizes of the reactor with the proposed design strategy. A pore wetness and surface perspiration model is proposed to explain the experimental data and rationalize the new design concepts. © 2011 American Institute of Chemical Engineers *AIChE J,* 58: 2820–2829, 2012

Keywords: Fischer–Tropsch, multiscale, gas to liquid, monolith, pore wetness, perspiration, catalyst design, reactor design, structure

Introduction

Syngas ($CO+H_2$) is mostly produced from fossil fuels such as petroleum, coal, and natural gas in current industrial processes. It can also be derived from various energy and carbon sources, such as biomass, industrial and agricultural wastes, municipal solid wastes, captured CO_2, and wind and solar power. Catalytic conversion of syngas is one critical process technology for the production of liquid hydrocarbon fuels and/or chemicals from those stranded and/or renewable resources. Fischer-Tropsch (F–T) synthesis is a well-known industrial process for conversion of syngas to hydrocarbon liquid fuels. However, a conventional F–T plant is typically operated at high processing capacities[1,2] and integrated into a petrochemical and/or refinery complex to achieve scale economy. By contrast, most renewable energy and/or remote hydrocarbon resources are characteristic of small capacities and unstable supplies, and they are distributed at wide geographic locations. The conversion process becomes cost-prohibitive by using the conventional process technologies and plant designs at such a capacity scale, that is, orders of magnitude smaller than the typical petrochemical plant or oil refinery. In addition to the capacity-scale economy, operational flexibility such as quick unit turn-around from shutdown to start-up is necessary for distributed conversion units. Stepout catalytic processing technologies are needed for distributed production of chemical feedstock and/or liquid fuels.

A great amount of research and development effort reported in the literature has been devoted to improvement of catalyst compositions and/or structures by utilizing new materials and state-of-the-art characterization tools. Examples in the catalyst design aspect are egg-shell catalyst beads for fixed beds,[3] cobalt-based catalysts,[4–6] iron-based catalyst,[7] catalyst particles for slurry reactors,[8] and new catalyst compositions of enhanced product selectivity.[9] The tubular fixed beds, fluidized beds, and slurry bubble columns are the commonly-employed reactor technologies.[10–13] Microchannel reactor concepts have been proposed and explored to enhance heat and mass transfer by making characteristic transport dimensions substantially smaller than those in the conventional tubular reactor.[14–16] Overall, the literature reports on new reactor design ideas/principles have been scarce relatively to catalysis studies.

The F–T reactor equipment itself represents only a fraction of the total capital cost in a conventional F–T unit,[17] while majority of the cost is associated with auxiliary systems and installation. Typically, the F–T reactor produces a reaction mixture effluent containing a significant fraction of unconverted syngas and by products such as methane in addition to the desired liquid product. The unconverted syngas has to be separated out of the product mixture and recycled back to the reactor. The recycling loop, heat exchangers, and/or catalyst recovery add to the unit complexity, and incurs more energy consumption and capital cost.

Correspondence concerning this article should be addressed to W. Liu at wei.liu@pnl.gov and weiliu2476@yahoo.com.

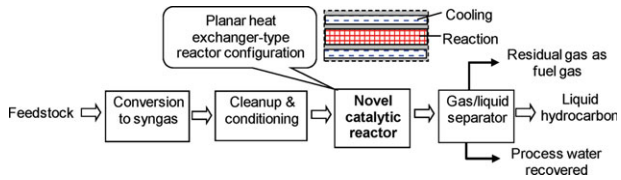

Figure 1. Simplified process flow diagram with proposed reactor technology.

[Color figure can be viewed in the online issue, which is available at wileyonlinelibrary.com.]

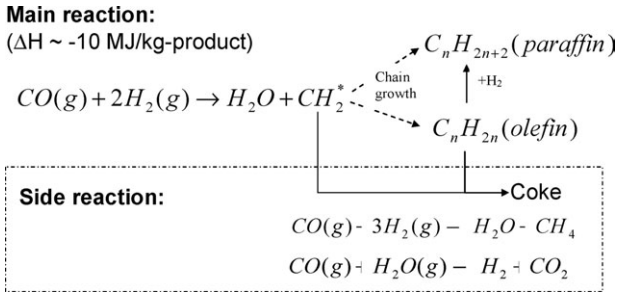

Figure 2. Major reaction paths under F–T reaction conditions.

Present Reactor and Catalyst Bed Design Concepts

The goal of our study is to develop a new reactor technology that enables essentially complete conversion of syngas in one pass without excessive production of methane and that leads to a compact unit suitable for small-scale operation. The proposed process flow diagram is illustrated in Figure 1. The reactor is run under such conditions that >90% of syngas feed is converted. In this way, the complicated gas recycling system is avoided. The reactor effluent is separated with relatively simple means into residual gas, liquid hydrocarbons, and water. The residual gas containing H_2, CO, methane, and CO_2 can be combusted as a fuel gas to provide energy to the unit operation, while the water can be reused in the syngas production process. The hydrocarbon mixture is lumped as one liquid-phase product that can be transported to a centralized location, such as a petrochemical plant or refinery, for production of specific liquid fuels and/or chemical products. The compact reactor unit can be standardized for mass production and be readily deployed to various geographic locations.

Obviously, the reactor design is a critical challenge to realize the above process objective. There must be good reasons why the current reactors are not run at complete one-pass conversion. To aid discussions of the proposed reactor design concept, a simplified reaction network is given in Figure 2 showing characteristic of the syngas catalysis chemistry. The F–T synthesis is a surface catalyzed polymerization reaction process that uses CH_x monomers, which are formed by hydrogenation of adsorbed CO molecules, to produce hydrocarbons with a broad range of chain length and functionality. In parallel to the desired polymerization reaction, methane can be produced by the methanation reaction, and water-gas-shift reaction may occur to produce CO_2. Coke can be produced from either CO decomposition or uncontrolled polymerization reactions. Coking often causes catalyst deactivation.[18,19] The F–T reaction is highly exothermic and can easily run away if the temperature is not effectively controlled. The F–T reaction occurs under an environment of multiple physical phases and complex chemical compositions, which could include liquid-phase hydrocarbons such as waxes, water, light hydrocarbons, inorganic gases (H_2, CO, CO_2), and solid catalysts. These are basic issues being considered for design and development of new reactor technologies.

In the authors' point of views, the limiting factors to run high one-pass conversion with conventional reactors could be (i) high CH_4 and CO_2 selectivity; (ii) balance between constraints of flow hydrodynamics and reactor operation; (iii) accelerated catalyst deactivation; (iv) lack of an effective catalyst; and (v) effective temperature control of the catalyst bed. Thus, a multiscale design strategy is presented in this work to tackle these long-standing problems by decoupling of convoluted factors.[20,21]

The proposed reactor design principles are illustrated with a modular reactor schematic shown in Figure 3. A monolithic-structured catalyst bed is employed in planar heat exchanger-type configuration. Each layer of the reaction zone is arranged adjacent to two heat exchanging zones. The layers can be repeated to the desired height. Different from the microreactor approaches, the spacing of a reaction zone in the proposed design may be ranged from 5 to 30 cm, i.e., at macroscales. Thus, existing material processing technologies can be utilized to fabricate such kind of reactor modules. The structured catalyst bed is the core of the reactor design. The structured bed comprises an array of parallel catalytic reaction channels of a channel size at 0.3 to 3.0 mm levels, which may be called as mini-channels. The mini-structured bed can be made by proven material processing methods, such as ceramic monoliths made by extrusion. A syngas feed stream is introduced into the catalyst bed from the top slit between the heat exchanging wall and top surface of the structured bed. The feed gas is distributed uniformly into individual catalyst channels as mini-streams by making 90-degree turn in its flow direction as the bulk gas flows along the slit. A porous membrane sheet may be placed on the top of the structured bed to serve as a gas distributor. The mini-gas stream flows downward through a catalytic reaction channel. The reacted product streams discharged from individual channels are collected at the bottom slit between the heat exchanging wall and the bottom surface of the catalyst bed. The resulting bulk product flow is discharged out of the reactor. The flow is driven by a positive pressure gradient between the inlet and outlet of the reactor module. The reaction heat generated from the catalyst bed is transported to the heat exchanging wall through convective flows in the feed and product slits.

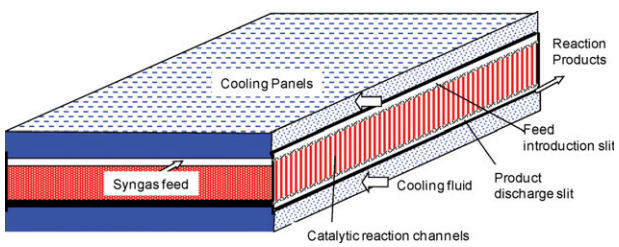

Figure 3. Schematic of multiscale engineered reactor module proposed in this work.

[Color figure can be viewed in the online issue, which is available at wileyonlinelibrary.com.]

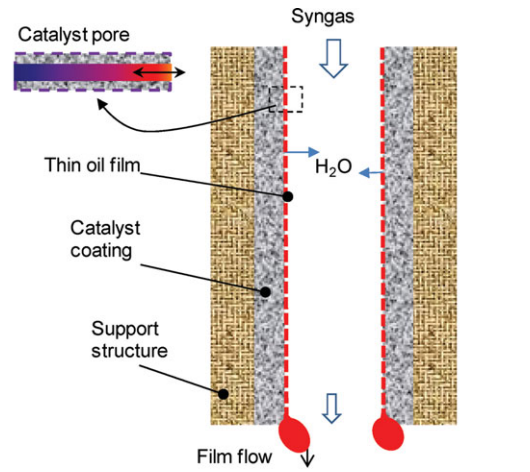

(a) Proposed pore wetness and surface perspiration model

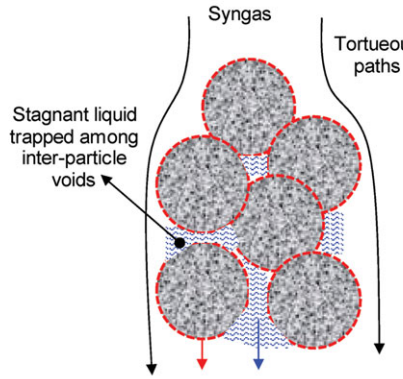

(b) Packed catalyst beads (or particles)

Figure 4. A model for structured bed of straight flow channels in comparison to particle-packed bed.

[Color figure can be viewed in the online issue, which is available at wileyonlinelibrary.com.]

This reactor design approach allows decoupling of design parameters at reactor-scale, reaction zone-scale, and catalyst channel scale. The reactor-scale design can address bulk flow distribution, cooling flow arrangement, heat exchange efficiency between the reaction and cooling layer, mechanical integrity of the reactor vessel, and thermal and pressure stresses of the reactor system. At the scale of a single reaction zone (or catalyst bed), the monolithic-structured bed serves both as a catalyst support and as a three-dimensional thermal conduction matrix. The reaction heat generated at a local reaction spot can be spread throughout the support by thermal conduction. Compared to point-to-point contacts in a conventional bead-packed catalyst bed, the continuous solid support structure should provide good thermal conduction. Thus, flow distribution, and mass and heat transfer issues in a reaction zone can be addressed by adjusting bed-scale design parameters, such as thermal conductivity of the support, open-frontal area fraction (or solid loading), channel size, and bed length.

The catalyst structure and mass transfer between the catalytic sites and the channel flow can be handled by the channel-scale design, which are illustrated with one representative reaction channel in Figure 4a. The structured bed design allows fabrication of catalyst wall structures independent of reactor designs, such as thickness, catalyst distribution along the thickness, and pore structures. The whole channel wall can be made of active catalysts, although a coated catalyst structure is shown in Figure 4a. The feed gas diffuses into the catalyst pore and reacts as it flows through the channel, and the produced liquid drips off the channel wall and comes out of the channel along with the gas flow. The flow pattern for the bead-packed fixed bed is illustrated in Figure 4b for comparison purposes.

As outlined in Figure 5, a series of elemental mass transfer steps are involved in an actual catalytic conversion process even at the channel scale. The reactants (CO and H_2) need to transport from the channel flow to the catalytic sites, while the reaction products (Oil, H_2O, CH_4) need to be transported from the catalytic sites back into the channel flow. The pore diffusion and catalyst loading can be managed by controlling thickness and pore structures of the catalyst coating layer, while the mass transfer from the channel flow onto the catalyst wall surface can be controlled by flow conditions (Ug, U_l) and channel geometry. A salient feature of the structured reaction channel[22] is the possibility to achieve uniform gas/liquid/catalyst contacting, plug flow, and high external mass transfer rates, as compared to the bead-packed bed and slurry bubble column. Both gas and liquid inside the channel move in one direction, typically along gravitational direction. The high aspect ratio (length/diameter) of a small-size channel further favours for a plug flow pattern. In the bead-packed bed, segregation of the gas and catalyst at the particle scale is inevitable due to random stacking of particles and trap of the liquid product among interparticle voids. In the bubble slurry column, the catalyst particles may be uniformly dispersed in the liquid-phase product, but there would be back-mixing of the product and syngas bypass.

Design parameters at the reactor and reaction-zone scales should be well simulated by computer modeling based on the design and material structures studied in the related fields, such as heat exchangers and diesel particulate filters. The catalytic channel reaction performance, which is the fundamental of the proposed reactor design, is experimentally tested.

Experimental Testing of Fundamental Design Ideas

Catalyst preparation

The CoRe/alumina catalyst is used in this work. Its formulation and preparation in powder or particle form was studied in our previous work.[15,23] There are several excellent publications around this catalyst system for F–T reactions regarding its preparation, characterization, and correlation of reaction performances with catalyst structures.[4–6] This work is mainly to study catalytic performances in a monolithic catalyst channel. By using the known catalyst formulation, we can focus on the catalyst preparation in a monolith structure.

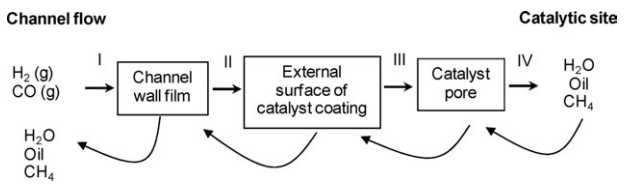

Figure 5. Elemental steps involved in a catalytic syngas conversion process.

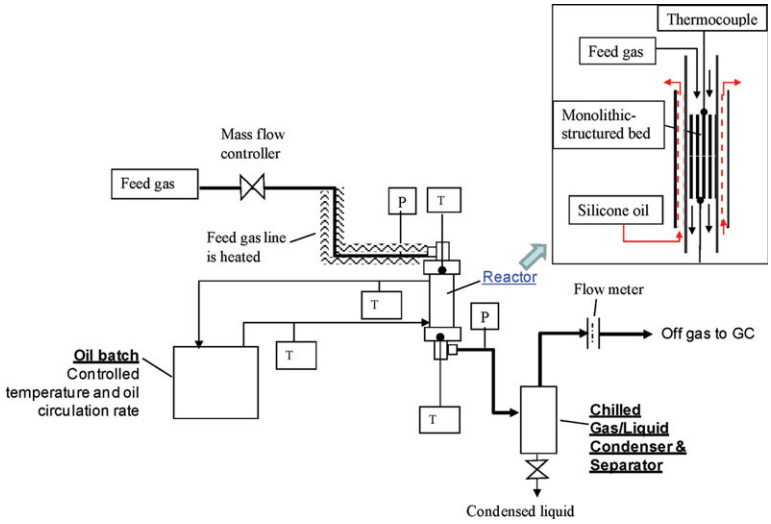

Figure 6. Schematic of reactor testing apparatus used in this work.

[Color figure can be viewed in the online issue, which is available at wileyonlinelibrary.com.]

The commercial cordierite monolith substrate was used to make the structured catalyst bed. Three major steps involved in the preparation of a monolithic catalyst were slurry batching, alumina coating, and catalyst impregnation. The alumina coating slurry was prepared in the following procedure. One hundred mesh of acidic Al_2O_3 powder (Engelhard) was mixed with deionized water. Polyacrylic acid (PAA) with molecular weight of 2000 g/mol (Sigma–Aldrich) was added as an electrostatic dispersant. pH of the slurry was adjusted within the range of 3–4 by adding HNO_3 solution. Then, polyvinyl alcohol (PVA) (Aldrich) and Lgepol C0-720 (Sigma–Aldrich) were added as a binder and surfactant, respectively. Furthermore, polyethylene glycol (PEG) (Sigma–Aldrich) with molecular weight of 2000 g/mol was added as a plasticizer. The resulting slurry batch had typical compositions of about 30 wt % alumina, 0.2 wt % PAA, 1.0 wt % PVA, 1.0 wt % PEG, and 0.1 wt % Lgepol. The whole mixture was ball milled for 16–48 hrs to obtain homogeneous slurry.

The slurry was coated on the monolith support of 1 cm diameter $\times$ 7.5 cm long by a dip coating technique, i.e., quick contacting of the monolith with the coating slurry. The coating was repeated three times with interstage drying at 100°C. Finally, the coated monolith was calcined at 550°C for 4 h at 5°C/min ramp rate for removal of all the organics and for adhesion of the alumina coating layer onto the support. On average, the alumina coating loading was 16.0 wt %.

The active catalyst metal was dispersed on the alumina coating with impregnation technique. The impregnation solution was prepared by dissolving cobalt nitrate hexahydrate (98% purity, Aldrich), perrhenic acid (Engelhard), and lanthanum nitrate hydrate into deionized water. The monolith was wetted by the solution. After excessive solution inside the channel was removed, the wetted monolith was dried in air at 90°C overnight and followed by calcinations at 350°C for 3 h. The impregnation was repeated to obtain targeted catalyst loadings. The resulting Co, Re, and La loading on the alumina coating was 17.8 wt %, 3.3 wt %, and 3.0 wt %, respectively. The total catalyst metal loading on the alumina basis was 24.1 wt %, while the catalyst loading (metal +alumina) in the whole monolith piece was 19.2 wt %.

For comparative testing, alumina-supported F–T catalyst particles were prepared by using the same raw materials, impregnation solutions, and drying and calcination conditions as described above.

Catalytic reaction tests

Schematic of the reactor system used in this work is shown in Figure 6. The monolith catalyst module was inserted into a $^1/_2$" OD reactor tube of suitable ID so that the gap between the tube wall and the monolith was comparable or less than the channel size. This way of packing was necessary to minimize bypass of the flow along the channel wall. The monolith catalyst was positioned in the middle of the reactor tube by two thermocouples at the top and bottom. Thus, no other material was loaded into the reactor during testing of monolith catalysts. The reactor tube was wrapped by an oil jacket to control the reaction temperature, and the temperatures were measured at the bottom and top of the catalyst bed.

For testing of catalyst particles, the catalyst particle was packed in the middle of a reactor tube by using SiC particles as diluents. Similar to the reactor configuration for the monolith catalyst bed, the thermocouple wells were placed at the top and bottom of the catalyst bed, respectively; and the reactor tube was sheathed in an oil jacket for temperature control.

All the catalysts were activated by reduction in hydrogen before introduction of the syngas. After the catalyst was reduced at about 400°C for 12 hours at 0.1 MPa of H_2, the reactor temperature was cooled down under flowing hydrogen. Then, the reactor was pressurized to 25 bars with 5% H_2 in helium. A syngas feed with H_2/CO ratio of 2, unless specifically noted, was introduced. Argon (3–4 vol %) was spiked into the feed both as an internal standard and for purge purpose. The reactor temperature was raised to the target value at 1°C/min. Hydrocarbon and water in the reactor effluent was condensed in a chilled vessel under pressure. Noncondensed gases were analyzed using an on-line gas chromatograph (Agilent QUADH G2981A with Molsieve 5A, PoraPlol Q) to determine CO conversion and light product selectivity. The condensed liquid products were analyzed in a HP 6890 connected with a DB-5 column. The olefinic

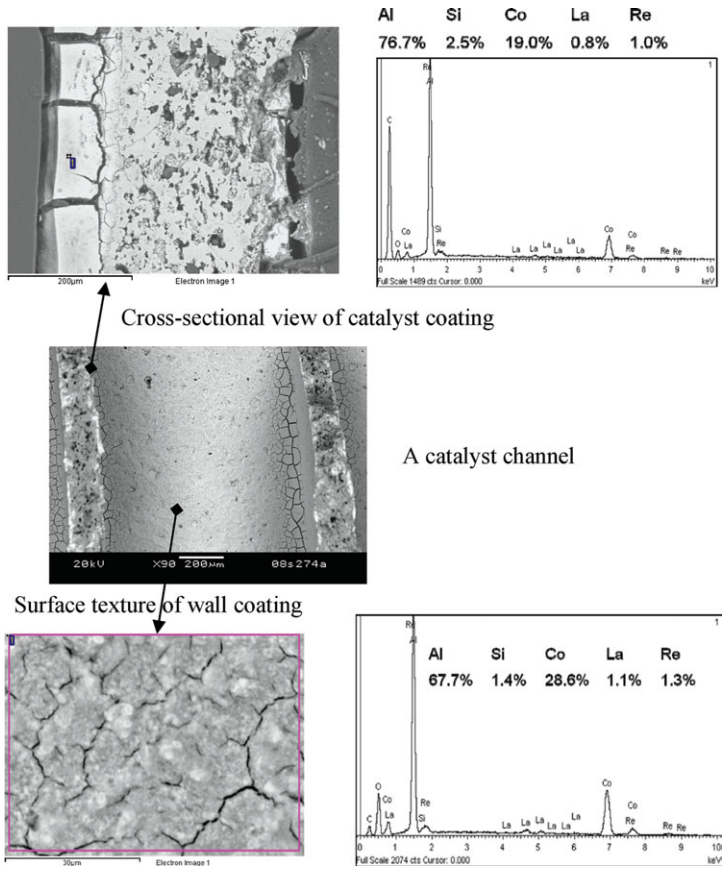

Figure 7. Structure and composition of F–T catalyst coating on Cordierite monolith channel.

[Color figure can be viewed in the online issue, which is available at wileyonlinelibrary.com.]

compounds were identified by GC-MS (HP 5973C), then quantified by a GC (HP 6890). Conversion and selectivity are calculated based on the product gas analysis for CO, CO_2, CH_4, C_2H_4, C_2H_6, C_3H_6, C_3H_8, and C_4.

CO conversion is calculated by the following equation

$$X_{CO} = \frac{F_{in,0} \cdot x_{CO,in} - F_{ex,0} \cdot x_{CO,ex}}{F_{in,0} \cdot x_{CO,in}} \quad (1)$$

Selectivity toward molecule i on carbon number basis is calculated as follows

$$S_i = \frac{F_{ex,0} \cdot x_{i,ex} \cdot n_i}{X_{CO} \cdot F_{in,0} \cdot x_{CO,in}} \quad (2)$$

Weight-hourly space velocity is calculated based on CO mass feed rate to characterize the catalyst activity

$$WHSV = \frac{m_{CO}}{W_{Cat}} \quad (3)$$

Superficial gas linear velocity based on the reactor entrance condition is used to characterize the channel flow conditions

$$U_g = \frac{F_{in,0} \cdot T_{top}}{T_0 \cdot P \cdot A_R \cdot 60} \quad (4)$$

Experimental Results and Discussion

Catalyst coating

Uniformity of the catalyst coating on the monolith support was examined by Scanning Electron Microscopy (SEM) and Energy-dispersive X-ray spectroscopy (EDS) analysis. The coating surface texture and cross-section are shown in Figure 7. The channel surface is fully covered by the catalyst coating, even though there are mud cracks on the coating. The catalytic reaction occurs inside meso-pores of the catalyst coating, which are invisible by SEM. Presence of a catalyst coating layer is also evident in the cross-sectional view. The channel opening is about 0.9 mm, while the catalyst coating thickness is about 30 to 70 μm. The EDS analysis shows presence of Al, Si, Co, Re, and La elements. The Al and Si are attributed to the support, while Co, Re, and La are impregnated catalyst metals. Presence of the catalyst metals on the channel wall surface and at the middle point of the coating depth is confirmed. The SEM/EDS analyses provide compositions at the localized spots. For a given global composition, variation of the compositions among different spots is possible.

Exceptional performances of the monolithic-structured catalyst bed

Steady-state reaction performances of the structured bed are shown by plots in Figure 8. First of all, the temperature control was excellent. Given about 150 mm of the bed height, the top and bottom temperatures of the catalyst bed

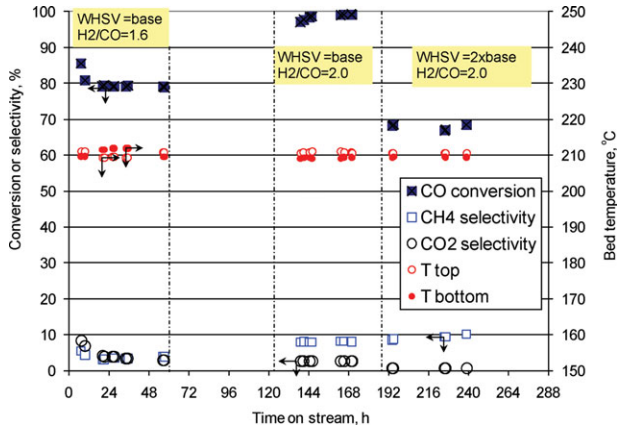

Figure 8. Steady-state performance of structured catalyst bed (25 bar).

[Color figure can be viewed in the online issue, which is available at wileyonlinelibrary.com.]

are consistent, and their differences are typically less than 2°C at high CO conversion levels. Superficially, one thought that the bottom bed temperature could be much higher than the top bed due to exothermic reactions in the confined catalyst channel. The small temperature difference observed from the experiments here can be explained by the thermal conduction through the monolith support matrix and rapid heat transfer between the silicone oil and reactor tube. The gap between the reactor tube wall and monolith body apparently did not impose limitation to the radial heat transfer. This result confirms the possibility of the temperature control at a larger spacing of the reaction zone in the proposed reactor design (Figure 3) than the diameter of conventional tubular reactors, certainly orders of magnitude larger than the microchannel reactor spacing.

The structured bed had a rapid response to changes of the reaction conditions, and showed fairly good stability. The steady-state reaction could be reached within a few hours. The possibility to reach high CO conversion levels without excessive production of CH_4 and CO_2 is clearly shown. The reactor was started with a syngas feed of $H_2/CO = 1.6$ containing 3.9 vol % Ar as an internal standard. Figure 8 shows about 79% CO conversion that corresponds to nearly complete H_2 conversion. The CO conversion higher than the stiochiometric (80%) during the transient period was due to the inventory hydrogen in the reactor system before the syngas introduction, since the catalyst was pre-reduced in pure H_2 gas. After the feed H_2/CO ratio was adjusted to stoichiometric ratio of 2.0, about 95–98% of CO conversion occurred under the same temperature, pressure, and space velocity. Since the CO conversion was so high, nearly all the feed H_2 and CO gas was consumed and we had difficulty to maintain the reactor pressure with a very small flow of remaining Argon gas. It should be noted that the methane and CO_2 selectivity were only about 8% and 2%, respectively. After the space velocity was doubled, under the same temperature and pressure, the CO conversion was dropped to about 68%, the CH_4 selectivity increased to about 9.5%, while the CO_2 selectivity decreased to less than 0.5%. Decline of the CO % conversion with increasing space velocity can be explained by reduced residence time. However, variations of the CH_4 and CO_2 selectivity with the space velocity could not be explained based on residence time.

After a few weeks of testing, this reaction run was quenched by switching the feed gas to an inert purge gas and by cooling down the reactor tube with cold silicone oil. The spent monolith catalysts were unloaded from the reactor tube for post analysis.

Reaction uniformity among monolith channels

For structured beds, uniform flow distribution and reaction in all catalyst channels is a critical factor for effective catalyst utilization and for minimization of side reactions. Thus, the above reaction testing was stopped in the middle of a steady-state run to examine the reactor tube and monolith catalyst. The pictures of two spent monolith pieces retrieved from the above reaction run are shown in Figure 9. The reactor tube itself was very clean after testing, and there were no coke and/or strange matters deposited on the tube wall. The two monolith pieces were intact. All the channels facing the feed syngas in the upper piece of the monolith catalyst were fully open. The monolith piece looked uniform, indicative to uniformity of the catalyst deposition and reaction. The monolith support without catalyst coating would look grey, and the white wax would be trapped if there was any stagnant or dead space. All the channels in the lower piece of the monolith were filled with white wax on the bottom, which confirms that the reaction (including formation of wax) occurred among all the channels as explained below.

The monolith catalyst channel surface was likely covered by a layer of long-chain hydrocarbon liquids (such as waxes) during steady-state reaction. After the feed gas was suddenly switched to an inert purge gas and the reaction bed

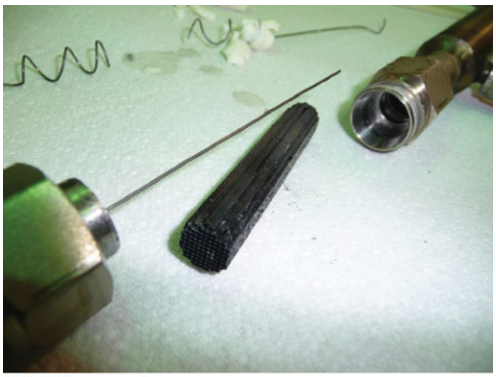

(a). Upper piece

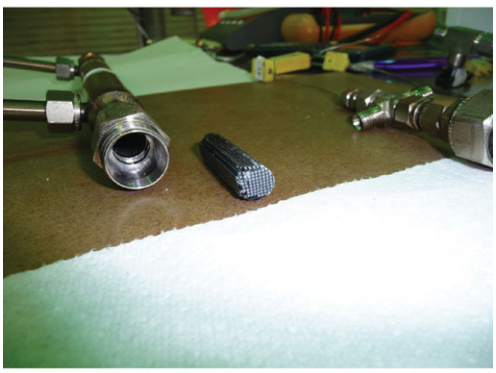

(b) Lower piece

Figure 9. Morphologies of monolith catalyst pieces after 45-day testing.

[Color figure can be viewed in the online issue, which is available at wileyonlinelibrary.com.]

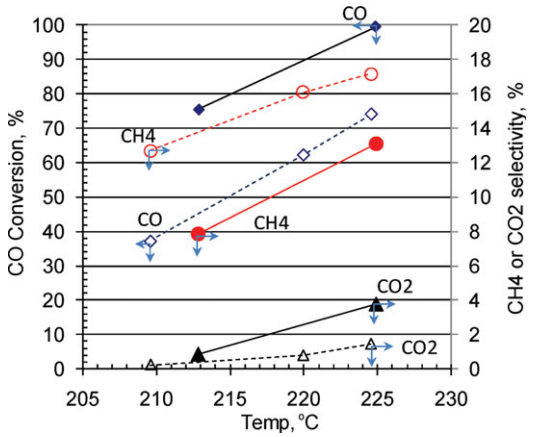

Figure 10. Impact of reaction temperature on performance of structured catalyst bed (feed H_2/CO ratio of 2:1, reactor pressure of 25 bar).

Closed symbols for WHSV = 2.0 h^{-1}. Open symbols for WHSV = 4.1 h^{-1}. [Color figure can be viewed in the online issue, which is available at wileyonlinelibrary.com.]

temperature was quickly cooled down, the liquid film on the channel surface gradually flowed downwards along the channel surface so that the liquid product was accumulated on the bottom of the monolith module. Since the catalyst bed was quickly cooled, solid wax was preserved at the bottom of the monolith channel. These observations suggest that the feed gas was distributed evenly among the catalyst channels by simple stacking of two pieces of the monolith catalyst modules.

Parametric tests of monolithic-structured catalyst bed and impact of gas superficial linear velocity

To elucidate reaction behavior of the structured bed, the reactor was loaded with two pieces of fresh monolith catalysts and tested under various reaction conditions. These two pieces of the catalyst were prepared in one group together with the other two tested above. The same preparation procedure and conditions were used. Thus, they were expected to be similar to what were used in the above run. The reaction testing was started and lined out with a feed gas of CO/H_2 ratio of 2 under the same conditions as used in the previous run. During 2-week lineout period, excellent temperature control and >95% one-pass CO conversion at (CH_4 +CO_2) selectivity less than 10% were shown. This run confirms reproducibility of exceptional performances of the present monolithic structured bed.

After a stable catalytic reaction performance was established, the reaction conditions were changed to assess their impact on the structured bed performance. Several data points were collected in a steady-state operation under each set of conditions, and the average values are reported here. Variations of CO conversion, CH_4 selectivity, and CO_2 selectivity with reaction temperature under constant reactor pressure are plotted in Figure 10. The temperature is taken as an average of the top and bottom bed readings. The closed symbols in Figure 10 are for WHSV of 2.0 h^{-1}, while the open ones correspond to WHSV of 4.1 h^{-1}. For a given WHSV, the CO conversion, CH_4 selectivity, and CO_2 selectivity all increase with the temperature. This is expected from simple reaction kinetics.

Comparison of the reaction performances at different WHSVs tells a different story. At the same temperature, the CO conversion and CO_2 selectivity decrease with increasing WHSV, which is as expected from the reaction kinetics. However, the CH_4 selectivity shows a very different behavior. At the same or similar temperature, the CH_4 selectivity increases with WHSV. Such a variation cannot be explained based on simple correlation of conversion with residence time.

The un-usual selectivity behavior is explained by effects of the channel flow hydrodynamics on the different reactions. The flow conditions inside the channel can be characterized by the gas superficial linear velocity under the reactor entrance conditions. It is recognized that the gas flow inside the channel would diminish while the liquid flow gradually increases along the channel depth. Thus, variations of CO conversion, CH_4 selectivity, and CO_2 selectivity are plotted vs. the superficial gas velocity in Figure 11. In these plots, the closed symbols and open symbols are for 225°C and 210°C reaction temperature, respectively. For a given temperature, the CO conversion decreases with increasing the gas velocity. This is explained by the reduced residence time, since the catalyst bed height was fixed. The CO_2 selectivity decreases with increase of the gas linear velocity. However, the CH_4 selectivity tends to increase with the gas linear velocity. The high CO conversion and low CH_4 selectivity are realized only at the low gas linear velocity.

Therefore, the gas linear velocity becomes one critical design parameter for the proposed reactor concept. The plate-like catalyst bed configuration as illustrated in Figure 3 would allow low gas linear velocities at high gas feed rates. The hydrodynamic pattern inside the catalyst channel could be very complex, due to presence of multiple phases. The proposed design allows scaling of the channel flow hydrodynamics from the small-scale laboratory reactor to practical sizes of the reactor.

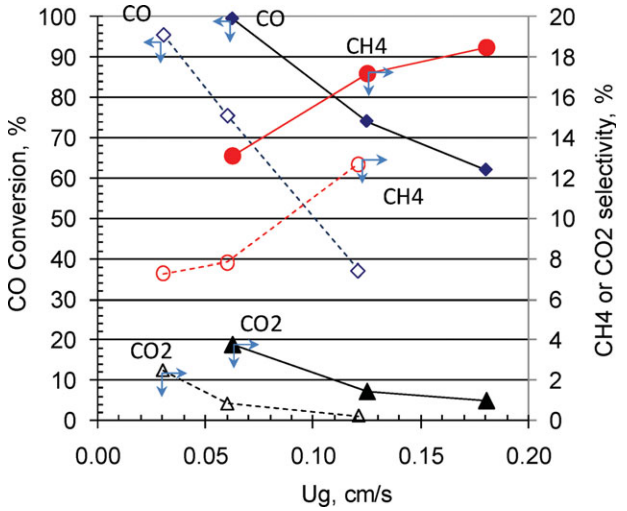

Figure 11. Impact of feed gas superficial linear velocity on performance of structured catalyst bed (feed H_2/CO ratio of 2:1, reactor pressure of 25 bar).

Closed symbols for reaction temperature of 225°C. Open symbols for 210°C. [Color figure can be viewed in the online issue, which is available at wileyonlinelibrary.com.]

Comparison of monolithic structured bed to its crushed particle bed

There is a great amount of literature studies about particle-packed beds for F–T reaction. It was reported in some earlier literature that CH_4 selectivity decrease and CO conversion increase could occur concomitantly by lowering space velocity of a given particle bed. However, the upper range of CO conversion in these studies was 80% for the unspecified particle bed[4] and up to 72% for a fixed bed packed with 53–90 μm catalyst particles,[5] which is lower than the 95–98% conversion levels reported above for the monolithic catalyst bed.

Various F–T catalyst particles were prepared and tested in a packed bed in this research laboratory previously. But, high CO conversion and low CH_4 selectivity were not obtained by trying various reaction conditions including space velocity. The best conversion results were achieved by packing a tiny reactor channel machined out of stainless steel (so-called microreactor) with fine catalyst particles.[15] The microreactor could not produce the kind of conversion results shown above for the structured catalyst bed, i.e., >90% CO conversion and <10% CH_4 selectivity.

To eliminate complication by possible catalyst variations, the monolithic catalyst pieces same as used above were crushed and sieved into particles of 60–200 mesh ($\sim$170 μm). The crushed monolith particle was loaded into a reactor tube and sandwiched by a layer of SiC particles on the top and bottom. The reactor was started and lined out in the same procedure as used above for the monolith bed. Different from the monolith bed, the crushed particle bed showed a rapid activity decline within first 24 h and reached a pseudo steady-state under constant reaction conditions after a few days. Then, reaction performances were measured by changing the conditions. Two or three data points were collected under each set of conditions. An average number is used to make plots.

The reaction performances of the crushed particle bed vs. the structured bed are compared in Figure 12. At the same reaction temperature of 210°C, Figure 12a shows that the structured bed gives much higher CO conversion than the crushed particle bed. The CO conversion activity of the monolith bed is about two to four times that of the crushed particle bed. The CH_4 selectivity of the crushed particle bed is fairly high relative to its low CO conversion level. The CH_4 selectivity decreases with increasing WHSV for the crushed particle bed, while an opposite trend is displayed for the monolith bed. Figure 12b shows that under constant space velocity, the CO conversion and CH_4 selectivity increase with temperature for both beds. Even though the space velocity for the structured bed is about two times of the crushed particle bed, the CO conversion with the structured bed is significantly higher than the crushed particle bed.

In conclusion, the un-usual performance obtained with the monolith-structured bed is not due to the catalyst material and calls for explanation by reaction engineering models.

Pore wetness and surface perspiration model for F–T reaction

This work reveals dramatic impacts of the catalyst bed design and operation conditions on F–T reaction performances for a given catalyst material. Clearly, the F–T reaction activity, selectivity, and stability are not merely a catalysis

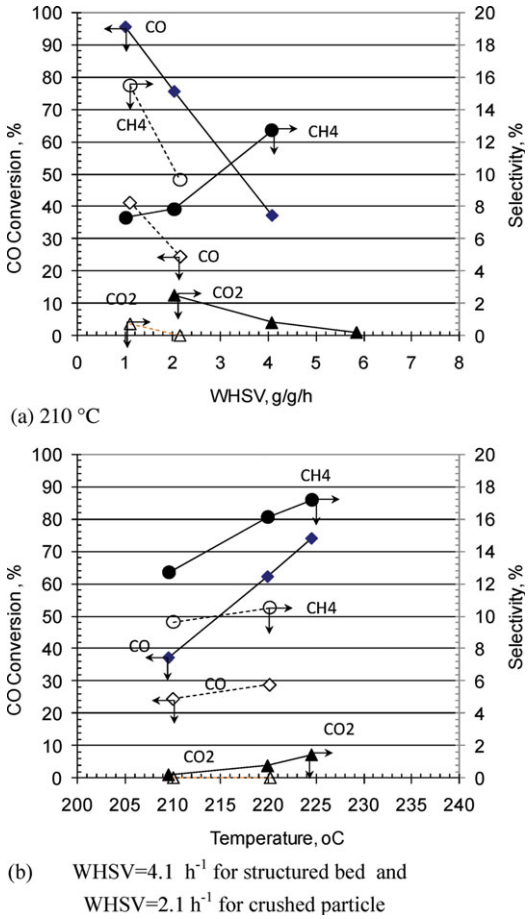

Figure 12. Comparison of monolith catalyst in structured bed to particle-loaded bed of its crushed particle (feed H_2/CO ratio of 2:1, reactor pressure of 25 bar).

Closed symbols for the structured bed. Open symbols for the particle bed. [Color figure can be viewed in the online issue, which is available at wileyonlinelibrary.com.]

problem, i.e., tailoring of catalyst pore structures, compositions and active sites. The ways how a catalyst is structured to contact with reactants inside a reactor and how the reactor is operated play a significant role in the resulting reaction performances. Based on our research results and literature analysis, we propose a simple model as depicted in Figure 4a to rationalize the catalyst bed designs for a high-performance F–T reactor. The design principles are elaborated in the following three aspects.

Structured Mini-Channel Flow to have a Plug Flow Pattern and Avoid Any Dead/Stagnant Space in the Bed. The plug flow is necessary to eliminate any back-mixing and achieve high one-pass conversion. Minimization of the dead space would also be helpful to prevent the catalyst deactivation from excessive reactions such as coking.

Fully-Wetted Catalyst Pores to Prevent the Catalyst Surface from Formation of Dry or Hot Spots. Methane formation on a dry catalyst can be very fast, due to fast gas diffusion and rapid heating up of the local spots. Methanation reaction can easily run away on a dry catalyst. When the catalyst pore is wetted by a liquid fluid, diffusion rates of H_2 and CO reactants are slowed down and thermal conductivity of the catalyst is significantly enhanced. F–T reaction

kinetics is slower than methanation. Thus, keeping the catalyst pore wetted would quench the methanation reaction without significant reduction of the F–T reaction rate. During a dynamic reaction process, the pore wetness is determined by the formation rate of the liquid product and drying (or liquid evaporation) rate. For a given temperature and pressure, the drying rate will be affected by the gas flow rate inside the channel. Thus, the gas linear velocity inside the channel should be controlled below a certain level to keep the catalyst surface stay wet. This mechanism explains the decreased methane selectivity with decreasing gas linear velocity, which is observed in this work. In other words, this model suggests that as long as the catalyst pore stays wetted, the side reaction of methanation could be curtailed.

Discharge of Reaction Products from Catalyst Pores Through Perspiration to have the Catalyst External Surface Covered Uniformly by a Thin Layer of Oil. The hydrocarbon and water molecules are continuously produced by the F–T reaction inside the meso-pores of the catalyst. The F–T reaction kinetics is relatively slow, and the produced hydrocarbon and water gradually diffuse out of the catalyst meso-pore onto the exterior catalyst surface – channel wall surface. The catalyst pore is so small that the hydrocarbon and water may be considered existing as a miscible phase inside the pore. Once they emerge on the channel wall surface, the water and hydrocarbon products would start to form its own phase, and the phase segregation occurs. The present authors speculate that the F–T catalyst surface would be more wettable by a hydrocarbon liquid than by water. Then, the hydrocarbon liquid product (or oil) is spread on the catalyst channel surface as a thin film, while the water product is either segregated off the channel wall as droplets or vaporized into the gas phase as water vapor, depending on its equilibrium partial pressure inside the channel. This process is similar to the perspiration of human body through the skin. The driving force for such a process is the surface tension and minimum Gibbs free energy.

Uniform coverage of the catalyst channel surface by a thin oil layer would protect the catalyst site from oxidation and/or leaching by possible condensed liquid water. The thin oil layer may also help fast mass transfer of H_2 and CO reactants on to the catalyst surface. This can explain a few times of the higher CO conversion activity obtained with the structured bed than with the crushed particle bed. Since the same catalyst material was used, the enhanced activity must result from enhanced external mass transfer of H_2 and CO, i.e., mass transfer from the bulk flow onto the catalyst external surface. The pore diffusion length in the structured bed should be the same as in the crushed particle, because the catalyst coating was fixed. Even though the crushed particle provides a much higher geometric surface area for external mass transfer than the channel surface in the structured bed, there could be a much smaller effective gas/liquid mass transfer area and/or thicker liquid film in the packed bed of the crushed particle than in the structured channel. As illustrated in Figure 4b, the liquid trapped in the interparticle voids may become stagnant so that there is no uniform gas/liquid/particle contact on individual particle basis. In a random-packed particle bed, the catalyst particles behave as an aggregate, cluster or a group. The equivalent size of such an aggregate would depend on the bed packing and reaction conditions, and could be orders of magnitude larger than the individual particle size.

The physical model presented here can be further delineated with mathematical equations in the future work. This reaction engineering model and the structured bed design concept should be applicable to syngas-to-liquid conversion processes other than the F–T reaction. Effective temperature control, high CO conversion activity, and low CH_4 selectivity are common performance characteristic for a gas-to-liquid conversion process. In this work, we use one catalyst material and monolithic support to elucidate the structured bed design ideas. The materials and structures of both catalyst and support can certainly be optimized to enhance the reaction performance of the structured bed. For example, a monolithic support of higher geometric surface area and more catalyst loading can be used to increase the reactor throughput. The monolithic support can be made of metallic or ceramic materials. Understandings of catalyst material designs in a monolithic structure bed comprise an interesting fundamental catalysis research subject.

Conclusion

Structured catalyst bed & reactor design concepts are presented in this work to address long-term dilemma for the gas-to-liquid catalytic reaction process, better temperature control, better catalyst activity and stability, lower CH_4 selectivity, ease for scale-up. For the given catalyst material and catalysis chemistry, all these problems are fundamentally related to mass and heat transfer at different scales. The proposed approach provides a way for decoupling of convoluted design parameters so that different aspects of the reactor design and operation problems can be tackled through designs at the reactor-scale, catalyst bed-scale, and individual channel-scale, respectively.

The fundamental idea of the proposed reactor design is demonstrated for the F–T catalytic reaction by using known catalyst and support materials, a Re-Co/alumina catalyst coated on a cordierite monolith support. At a H_2/CO feed ratio of 2, ~95% CO conversion and <10% CH_4 selectivity was obtained with the monolithic-structured bed. The structured bed shows about a few times of higher CO conversion activity than the crushed particle bed of the same monolith catalyst. These levels of high CO conversion and low CH_4 selectivity could not be obtained by using the conventional particle bed. The gas superficial linear velocity was found as one critical design and operation parameter for the structured bed. This finding suggests that the reaction performance be scalable from the laboratory testing unit to practical sizes of the reactor by maintaining the same gas superficial linear velocity (or hydrodynamics) inside the channel.

The pore wetness and surface perspiration model is proposed to explain the present experimental results and observations, and to rationalize new reactor designs for gas-to-liquid reaction processes.

Acknowledgments

The authors thank their former colleague, Dr. John Hu, for initial research work around F–T catalytic reactions. This work was supported under laboratory-directed research and development (LDRD) program of PNNL by Energy Conversion Initiative and Energy & Environmental Directorate. Pacific Northwest National Laboratory (PNNL) is operated by Battelle for the Department of Energy.

Notation

A_R = cross-sectional area of reactor tube, cm^2
$F_{in,0}$ = feed gas flow rate under standard gas conditions, sccm
$F_{ex,0}$ = residual gas flow of reactor effluent after the liquid condenser, sccm
m_{CO} = mass flow rate of CO fed into the reactor, g/h

n_i = number of carbon atoms in molecule specie i, i = 1 for CO_2 and CH_4.
P = reactor pressure, bar
S_i = selectivity toward gas specie i, i = CH_4, CO_2, C_2H_4, C_2H_6, C_3H_6, or C_3H_8
T_{top} = reactor top bed temperature, K
T_0 = temperature under standard gas conditions, 293 K
U_g = superficial gas linear velocity under reactor entrance conditions, cm/s
W_{cat} = net catalyst weight (alumina + metals), g
$x_{CO,ex}$ = molar fraction of CO in residual gas
$x_{CO,in}$ = molar fraction of CO in feed gas
$x_{CO,in}$ = molar fraction of CO in feed gas
$x_{CO,ex}$ = molar fraction of CO in residual gas
$x_{i,ex}$ = molar fraction of molecule i in residual gas
X_{CO} = conversion of CO

Literature Cited

1. Hoek A. 2003. The shell middle distillate synthesis process facts, technology and perspective. Presented at the CatCon2003, Houston, May 5–6th.
2. Sehabiague L, Lemoine R, Behkish A, Heintz YJ, Sanoja M, Oukaci R, Morsi BI. Modeling and optimization of a large-scale slurry bubble column reactor for producing 10000 bb/day of Fischer-Tropsch liquid hydrocarbons. *J Chin Inst Chem Eng*. 2008;39:169–179.
3. Iglesia E, Soled SL, Baumgartner JE, Reyes SC. Synthesis and catalytic properties of eggshell cobalt catalysts for the Fischer-Tropsch synthesis. *J Catal*. 1995;153:108–122.
4. Iglesia E. Design, synthesis, and use of cobalt-based Fischer-Tropsch synthesis catalysts. Fischer-Tropsch synthesis over gamma-alumina-supported cobalt catalysts: Effect of support variables. *Appl Catal A: Gen*. 1997;161:59–78.
5. Borg Ø, Eri S, Blekkan EA, Storsæter S, Wigum H, Rytter E, Holmen A. Fischer-Tropsch synthesis over gamma-alumina-supported cobalt catalysts: Effect of support variables. *J Catal*. 2007;248:89–100.
6. Jacobs G, Chaney JA, Patterson PM, Das TK, Davis BH. Fischer-Tropsch synthesis: study of the promotion of Re on the reduction property of Co/Al2O3 catalysts by in situ EXAFS/XANES of Co K and Re L edges and XPS. *Appl Catal*. 2004;264:203–212.
7. Dasgupta D, Wiltowski T. Enhancing gas phase Fischer-Tropsch synthesis catalyst design. *Fuel*. 2011;90:174–181.
8. Bukur DB, Carreto-Vazquez VH, Victor H, Ma WP. Catalytic performance and attrition strength of spray-dried iron catalysts for slurry phase Fischer-Tropsch synthesis. *Appl Catal A*. 2010;388:240–247.
9. Zhang QH, Kang JC, Wang Y. Development of novel catalysts for Fischer-Tropsch synthesis: tuning the product selectivity. *ChemCatChem*. 2010;2:1030–1058.
10. Sie ST, Krisha R. Fundamentals and selection of advanced Fischer-Tropsch reactors. *Appl Catal A*. 1999;186:55–70.
11. Hulet C, Clement P, Tochon P, Schweich D, Dromard N, Anfray J. Literature review on heat transfer in two- and three-phase bubble columns. *Int J Chem React Eng*. 2009;7:Art. No. R1.
12. Lu XJ, Hildebrandt D, Liu XY, Glasser D. Making sense of the Fischer-Tropsch synthesis reaction: start-up. *Ind Eng Chem Res*. 2010;49:9753–9758.
13. Zhu XW, Lu XJ, Liu XY, Hildebrandt D, Glasser D. Study of radial heat transfer in a tubular Fischer-Tropsch synthesis reactor. *Ind Eng Chem Res*. 2010;49:10682–10688.
14. Lee M, Rumbold SO. Industrial microchannel devices–where are we today? First International Conference on Microchannels and Minichannels, ICMM2003–1101, Rochester, New York, April 24–25, 2003.
15. Cao C, Hu J, Li S, Wilcox W, Wang Y. Intensified Fischer-Tropsch synthesis process with microchannel catalytic reactors. *Catal Today*. 2009;140:149–156.
16. Knochen J, Guttel R, Knobloch C, Turek T. Fischer-Tropsch synthesis in milli-structured fixed-bed reactors: experimental study and scale-up considerations. *Chem Eng Process*. 2010;49:958–964.
17. Naqvi S. Advanced Gas-to-Liquid Process. SRI Consulting, October 2006.
18. Tsakoumis NE, Ronning M, Borg O, Rytter E, Holmen A. Deactivation of cobalt based Fischer-Tropsch catalysts: a review. *Catal Today*. 2010;154:162–182.
19. Nam I, Seo JG, Hwang S, Song IK. Deactivation behaviors of hybrid Fischer-Tropsch catalysts in the production of middle distillate from synthesis gas in a dual-bed reactor. *Res Chem Intermed*. 2010;36:685–692.
20. Li J, Kwauk M. Exploring complex systems in chemical engineering—the multi-scale methodology. *Chem Eng Sci*. 2003;58:521–535.
21. Liu W. Multi-scale catalyst design. *Chem Eng Sci*. 2007;62:3502–3512.
22. Liu W. Mini-structured catalyst bed for gas-liquid-solid multiphase catalytic reaction. *AIChE J*. 2002;48:1519–1532.
23. Liu W, Hu J, Wang Y. Fischer-Tropsch synthesis on ceramic monolith-structured catalysts. *Catal Today*. 2009;140:142–148.

Manuscript received Mar. 29, 2011, and revision received Sep. 30, 2011.